Chapter 4

Spectral and NLO characteristics of Self assembled films of ZnO

Abstract

The third order nonlinear optical properties of self assembled films formed from ZnO colloidal spheres are investigated and are compared with those of ZnO thin films deposited by sol-gel process as well as pulsed laser ablation. ZnO thin films clearly exhibit a negative nonlinear index of refraction at 532 nm and the observed nonlinear refraction. The colloids and films developed by dip coating as well as pulsed laser ablation exhibit induced absorption whereas the self assembled film exhibits saturable absorption. These different nonlinear characteristics can be mainly attributed to the saturation of linear absorption of the ZnO defect states and electronic effects when the colloidal solution is transformed into self assembled films. ZnO colloids and self assembled films show two emission bands. The presence of pronounced visible fluorescence in the self assembled film confirms the presence of surface defect sates. We also report our investigations on the intensity, wavelength and size dependence of saturable and induced absorption of ZnO self assembled films and colloids. Values of the imaginary part of third order susceptibility are calculated for particles of size in the range 20-300 nm at different intensity levels ranging from 40 to 325 MW/cm^2 within the wavelength range of 450–650 nm. The wavelength dependence of figure of merit, which specifies the magnitude of nonlinear absorption for unit value of linear absorption, is calculated and this helps in comparing the absorptive nonlinearities at various excitation wavelengths.

The results of this chapter are published in

Litty Irimpan et.al., Optics Communications, **281**, 2938 (2008)

Litty Irimpan et.al., Applied Physics B: Lasers and Optics, **90**, 547 (2008)

4.1 Introduction

The search for new nonlinear optical materials with high optical nonlinearities is gaining interest both from research as well as industrial point of view. The essential requirements of good photonic materials are their large and ultrafast nonlinearity, synthetic flexibility and ease of processing. In recent years, wide bandgap semiconductors have been subjected to extensive studies because of the rising interest in the development of new nonlinear optical materials for potential applications in integrated optics. Impressive progress has been made in fabricating nonlinear optical waveguides from several nonlinear optical single crystals, which tend to be rather expensive. ZnO is an interesting wurtzitic II-VI wide bandgap semiconductor combined with high excitonic gain and large excitonic binding energy[1]. The optical properties of this material are currently the subject of tremendous investigations, in response to the industrial demand for optoelectronic devices that could operate at short wavelengths. There is a significant demand for thin film nonlinear optical materials, which can be integrated into an optoelectronic device. Recent studies have revealed that ZnO based self assembled films can act as photonic crystals.

Photonic crystals show a great deal of application in numerous types of devices in 1, 2, and 3D structures. Due to its promising applications such as integrated optical circuits and thresholdless lasers, photonic crystals have been extensively investigated[2]. Numerous techniques have been devised in an effort to produce periodic arrays of dielectric materials that can exhibit a photonic stop band. The fabrication of photonic crystals that work in the visible or near-infrared range is still a challenging topic. The principal method involves semiconductor fabrication technology, which includes lithography, layering, and etching processes. Several sophisticated methods have been developed, but they require expensive and large scale equipment[3]. One of the simplest techniques of fabricating photonic crystals involves

colloidal self-assembly, wherein, monodisperse colloidal spheres will spontaneously assemble into periodic arrays under certain circumstances. Zinc Oxide is a promising candidate for optically active self assembled photonic crystals[4].

Most of the work performed in the area of self-assembled 3D photonic crystals has involved a few materials which are readily available as monodisperse colloidal spheres in sizes appropriate for photonic crystals including SiO_2 and polymers, such as polystyrene and PMMA[5]. In addition, while some studies have been performed in which emissive materials are added to the photonic crystal matrix[6], no work has explored the properties of photonic crystals formed directly from optically active materials. Van Blaaderen et al. have produced a number of interesting emissive materials such as monodisperse colloidal spheres including Er^{3+} doped SiO_2, dye-doped PMMA, and SiO_2/ZnS core/shell structures[7]. ZnO is a promising candidate for optically active self-assembled photonic crystals because of its higher refractive index (2–2.2 in the visible regime) compared to other materials (1.4–1.5 for SiO_2 and most polymers). In addition, ZnO has been found to be an efficient emitter[8], exhibiting lasing behavior in the near UV region ($\lambda \approx 385$ nm).

Accordingly, designing novel ZnO material and, in particular, well defined anisotropic and highly oriented 3D large arrays is of great importance for fundamental research as well as for various fields of industrial and high technology applications. The thermodynamically stable crystallographic phase of this polar non-transition metal oxide is wurtzite and occurs in nature as the mineral Zincite (although scarcely as natural single crystal). ZnO has a hexagonal lattice, with an a:c axial ratio of 1:1.6. Its ionic and polar structure can be described as a hexagonal close packing (HCP) of oxygen and zinc atoms in point group 3m and space group $P6_3mc$ with zinc atoms in tetrahedral sites[9]. The occupancy of four of the eight tetrahedral

sites of HCP arrays controls the structure. The hexagonal unit cell contains two formula units, and the crystal exhibits a basal polar plane (001h) and two types of low-index faces, a nonpolar (1h00) face (and *C*6V symmetric ones) and a tetrahedron corner-exposed polar (001) face. The "low-symmetry" nonpolar faces with 3-fold coordinated atoms are the most stable ones. Additionally, there is no center of inversion in the wurtzite structure, and therefore, an inherent asymmetry along the *c*-axis is present allowing the growth of anisotropic crystallites[10].

An intense radiation can induce a profound change on the absorption property of a material, resulting in the intensity dependent transmittance, which is the so called nonlinear absorption[11]. Nonlinear absorption can be classified into two types: (i) transmittance increases with increasing optical intensity; this case corresponds to the well known saturable absorption (SA); (ii) transmittance reduces with increasing optical intensity; this type corresponds to induced absorption which includes two photon absorption (TPA), multiphoton absorption, and reverse saturable absorption (RSA). Different effects originating from different physical mechanisms can lead to a variety of different applications. For instance, SA materials have been used extensively in short-pulsed laser generations[12] as crucial passive mode-locking or *Q*-switching elements. Thus, it is paramount to fully characterize saturable performance, in which a typical figure of merit is the saturable intensity. SA characteristics depend on the inherent properties of a material and the parameters such as wavelength, intensity, and pulse duration of the laser used. To characterize nonlinear absorption, the open aperture *z*-scan technique, which was first pioneered by Sheik-Bahae *et al.*, has been extensively used[13]. Recently, an open aperture z-scan theory for the materials with simultaneous two and three photon absorption has been developed, which allows us to identify and determine the two and three photon absorption coefficients from a single open aperture z-scan trace[14]. The SA

properties of some materials are observed experimentally and analyzed theoretically[15]. The theory allows a straightforward estimation of the saturable intensity using the SA model for a material by fitting the experimental data. We also discuss the possible mechanisms of SA. When experiment on the characterization of the saturable absorption is performed by using a pulsed laser, if the nonlinear response time of the samples is much shorter than the laser pulse width, one can assume that the nonlinear effect depends on the instantaneous intensity inside the sample.

The studies on nonlinear processes in photonic materials are significant in the context of their technological applications, especially in areas such as passive optical power limiting, optical switching, and the design of logic gates. However, the switching to saturable absorption in ZnO self assembled films from induced absorption in colloids have not been explored and reported yet. In this chapter, we report our investigations on the size, intensity and wavelength dependence of saturable and induced absorption of ZnO self assembled films and colloids using 10 Hz, 5-7 ns pulses from a tunable laser by z-scan method[16-17]. Values of the imaginary part of third order susceptibility are calculated for particles of size in the range 20-300 nm at different intensity levels ranging from 40 to 325 MW/cm^2 within the wavelength range of 450–650 nm.

4.2 Theory

An intense radiation can induce a profound change on the absorption property of a material, resulting in the intensity dependent transmittance called nonlinear absorption[11]. The propagation through the sample is given by

$$\frac{dI}{dz} = -\alpha(I)I \qquad (4.1)$$

where $\alpha(I)$ is the intensity dependent absorption coefficient. z and

I are the propagation distance and the optical intensity inside the saturable absorption sample, respectively

Nonlinear absorption can be classified into two types: (i) transmittance reduces with increasing optical intensity corresponding to induced absorption; (ii) transmittance increases with increasing optical intensity corresponding to saturable absorption (SA)

4.2.1 Induced absorption

Induced absorption is characterized by decrease of transmittance with increase of the input energy. TPA is also referred to as induced absorption and there are various mechanisms leading to this process[13]. In the presence of TPA, the optical nonlinearity is described by the equation

$$\alpha(I) = \alpha_0 + \beta I \tag{4.2}$$

where α_0 and β are the linear and nonlinear absorption coefficients respectively.

4.2.2 Saturable absorption

Saturable absorption is characterized by an inecrease in transmittance with increase in input energy. When the beam propagates through a thin saturable absorber, the optical nonlinearity is described by the equation[16],

$$\alpha(I) = \frac{\alpha_0}{1 + \left(\frac{I}{I_S}\right)} \tag{4.3}$$

where I_S is the saturation intensity. Substituting this in equation (4.1) and integrating between the limits I_0 to I_L gives

$$\ln \frac{I_L}{I_0} = -\alpha_0 L - \left(\frac{I_L - I_0}{I_0}\right) \tag{4.4}$$

This can be solved numerically to get the transmission of the sample, I_L. If excitation intensity I_0 is greater than I_S, we can consider SA as a third order

process and in such cases $-\alpha_0 / I_S$ is equivalent to nonlinear absorption coefficient β which will then give $\mathrm{Im}(\chi^{(3)})$.

4.3 Synthesis

4.3.1 self assembled films of ZnO

Zinc Oxide is a promising candidate for photonic devices. Colloids of nano ZnO for the present studies are synthesized by a modified polyol precipitation method[16-17] as described in chapter 2. One of the simplest techniques of fabricating photonic crystals of ZnO involves colloidal self-assembly, wherein, monodisperse colloidal spheres will spontaneously assemble into periodic arrays under certain circumstances. Films are then produced from the ZnO colloidal spheres using a sedimentation self assembly process by the technique of drop casting onto a pre-heated glass substrate maintained at a temperature of 120^0C.

4.3.2 Thin films of ZnO through sol-gel process

In this method, deposition is carried out by the sol gel technique on commercially available glass substrate by the process of dip coating[17]. A stable hydrolysed solution is prepared using stoichiometric quantities of zinc acetate dissolved in diethanolamine and a cleaned substrate is immersed into this solution for thirty seconds at a controlled rate of 5 cm/min. The film is then kept for drying in a furnace for nearly 15 minutes at a temperature of 150^oC and annealed for half an hour at a temperature of 600^0C, to get good quality crystalline homogenous oxide films.

4.3.3 Thin films of ZnO through pulsed laser ablation

ZnO films are prepared by laser ablation of sintered ZnO target in the presence of an ambient gas at room temperature and a pressure of 500 mbar using the second harmonic of a Q-switched Nd:YAG laser[17]. The second harmonic beam from the Nd:YAG laser provide 300 mJ pluses of 7

ns pulse width at a repetition rate of 10 Hz. The laser beam is focused using a spherical convex lens on to the surface of the sample kept inside a stainless steel vacuum chamber through a glass window. The target is fixed at an angle of 45^0 with respect to the laser beam and is rotated at a constant rate during laser deposition, so that pitting of the target surface by the laser beam is uniform. The chamber gas environment during pulsed laser deposition (PLD) consisted of an oxygen partial pressure of 0.008 mbar and the deposition is carried out for duration of one hour at a laser beam power of 50mW.

4.4 Absorption spectroscopy

Figure 4.1(a) gives the room temperature absorption spectra of the ZnO colloid and self assembled film of size 20 nm and figure 4.1(b) shows that of ZnO thin films.

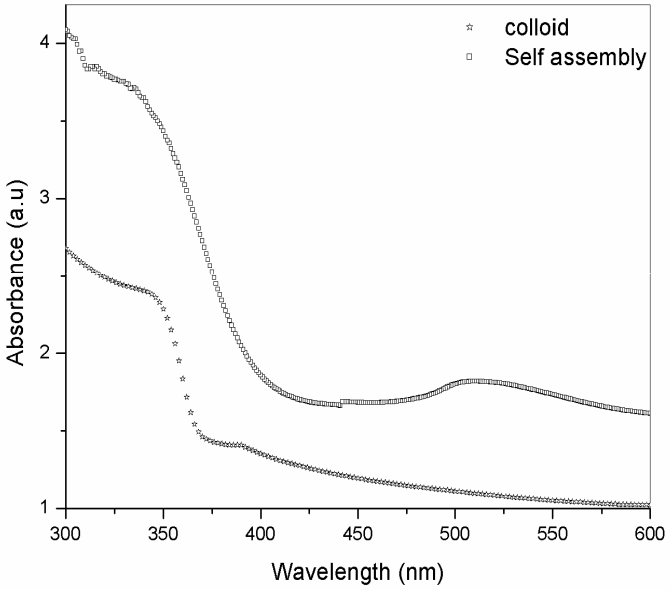

Figure 4.1(a): Absorption spectra of ZnO colloid and self assembled film

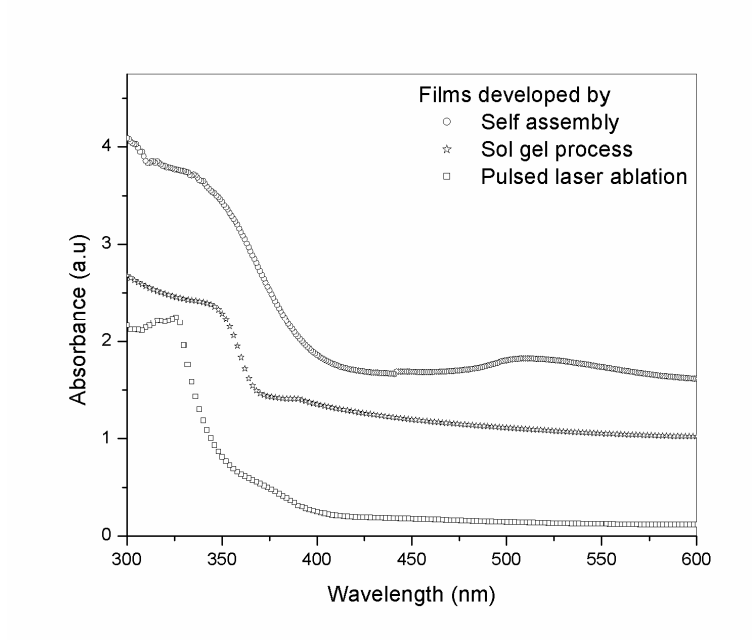

Figure 4.1(b): Absorption spectra of ZnO films

The excitonic peak of the colloid and the films developed by dip coating as well as pulsed laser ablation is found to be blue shifted from that of the bulk ZnO and can be attributed to the confinement effects[18]. The breadth of the absorption edge of the self assembled film indicates that there exists defect-related transitons[16-17]. Defects usually create discrete electronic states in the bandgap, and therefore influence both optical absorption and emission processes. The two most common defects in ZnO are likely to be oxygen and zinc vacancies and the visible band in the absorption spectrum can be related to the presence of these defect states in the self assembled film.

4.5 Optical bandgap

The direct bandgap are estimated from absorption spectrum as described in chapter 2.

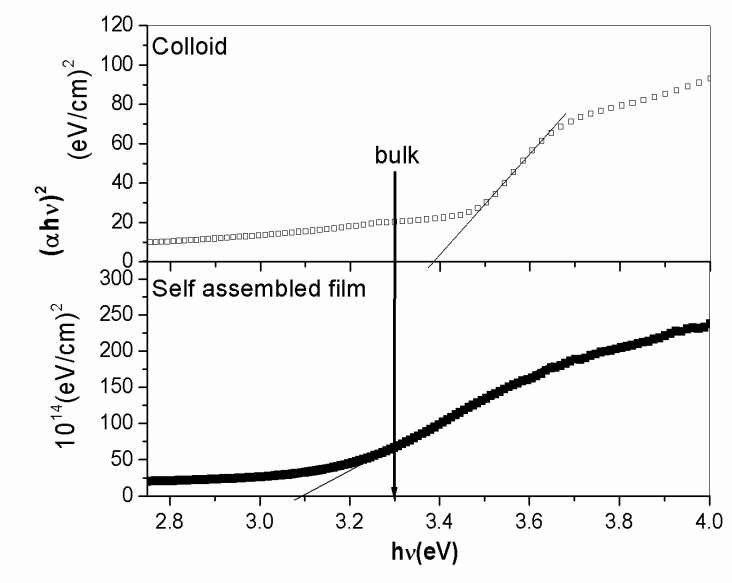

Figure 4.2(a): Optical bandgap of ZnO colloid and self assembled film

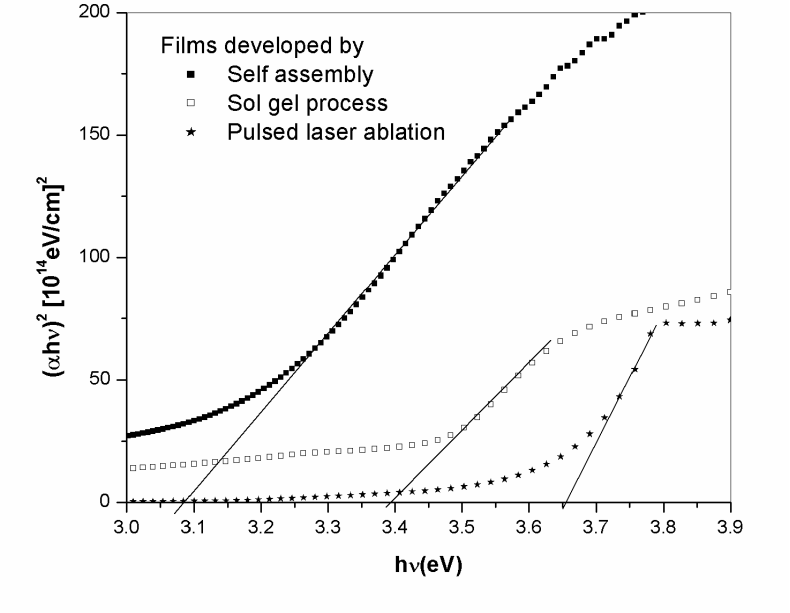

Figure 4.2(b): Optical bandgap of ZnO thin films

The optical bandgap (E_g) of colloidal and films of ZnO is found to be shifted from that of the bulk as shown in figure 4.2. The bandgap of self assembled film is reduced to 3.1eV from that of bulk (3.3 eV) whereas the bandgap energy of the colloid and that of the films developed by dip coating as well as pulsed laser ablation are higher than that of the bulk[16-17].

4.6 X-ray diffraction

The self assembled film and powder extracted from the colloid are characterized by x-ray diffraction. Typical XRD pattern of self assembled film is shown in figures 4.3. The XRD pattern of powder extracted from ZnO colloid is shown in chapter 2. The diffraction pattern and interplane spacings can be well matched to the standard diffraction pattern of wurtzite ZnO, demonstrating the formation of wurtzite ZnO nanocrystals. The particle diameter d is calculated using the Debye–Scherer formula[19] as described in chapter 2. The XRD peak at 36° gives the ZnO particle diameter of 18 and 20 nm for the colloid and film respectively.

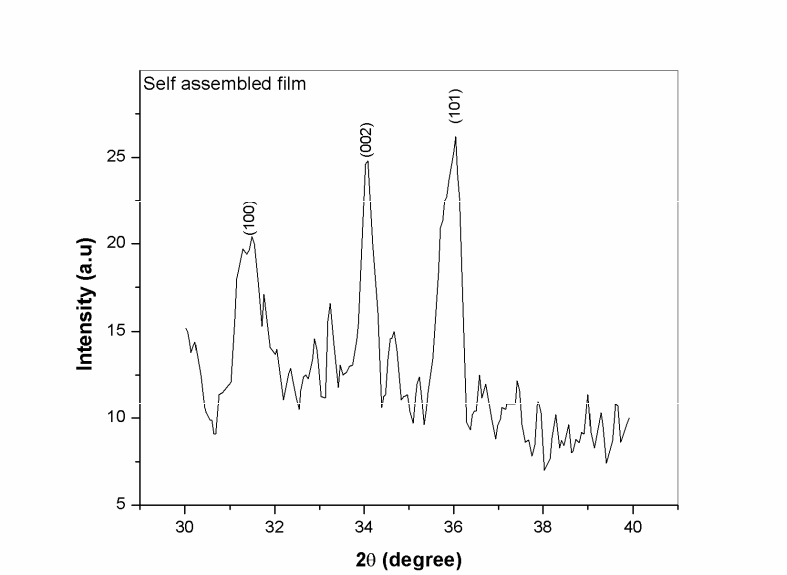

Figure 4.3: XRD pattern of ZnO self assembled film

Both colloid and film show three major orientations, viz., (100), (002) and (101). The (101) orientation is reported to be the prominent peak having the lowest surface energy and other orientations require more thermal energy to develop. The (002) direction is not the direction of fastest growth for ZnO. This we infer from the fact that the (002) faces of ZnO are the ones with the highest surface energy and these faces, according to basic crystal growth theory should, therefore, be among the faces of lowest growth rate[20]. But the relative intensity for the (002) orientation in self assembled film is observed to be higher compared to the colloidal spheres. In lattice mismatched epitaxial growth, it is well known that the increase of the length of *c* axis causes the decrease of the length of *a* axis. This means that ZnO thin film has a tensile built-in strain and this can be relaxed by providing sufficient thermal energy[20].

The (002) peak is observed at a diffraction angle (2θ) of 34.45^0 in the powder extracted from colloid and its line width is about 0.60. The diffraction angle from the (002) plane of bulk ZnO powder[21] is 34.4^0 and its line width is 0.20. On the other hand, the diffraction angle from the (002) plane of self assembled film is 34.06^0 and its linewidth is 0.80. Thus for self assembled films, a shift of the (002) diffraction angle towards lower angles and an increase in linewidth are also observed. Considering all these observations and the reduction of bandgap of self assembled films, we can conclude that there exist a strong correlation between the electronic structure and the geometrical structure of the ZnO arrays.

The crystallinity of self assembled film is poor compared to powder. Earlier observations have revealed that crystallinity of ZnO thin film was improved by annealing at high temperatures. Hence it is possible to develop other orientations by annealing at high temperatures and the mechanical properties of the self assembled film can be improved after heat treatment. Although ZnO self assembled films can act as photonic crystals,

unfortunately, we are not able to observe photonic crystal. Optimization of self assembled films to get photonic crystals is one of the promising areas for future works.

4.7 Scanning electron microscopy

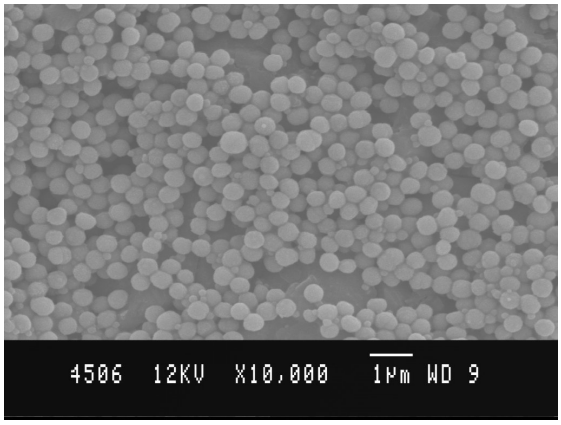

Figure 4.4: SEM image of ZnO self assembled film on silica substrate

To compare the monodispersity of the self assembled colloidal spheres with the actual values, the structure of the self assembled films is recorded using a scanning electron microscope (SEM, S-4300 Hitachi). The SEM image for a self assembled film on silica substrate is shown in figure 4.4 which indicates the presence of monodispersed ZnO spheres with an average particle size of 300 nm.

4.8 Fluorescence spectroscopy

Figure 4.5 shows the fluorescence spectra of ZnO colloid and self assembled film of size 20 nm for an excitation wavelength of 325 nm. From the figure it is clear that two emission bands are present, a UV emission band and another in the green region[16-17]. The UV band has been assigned to the bandgap fluorescence and the visible band is mainly due to surface defect states. The presence of pronounced visible fluorescence in the self assembled film confirms the origin of 530 nm emissions due to the presence of surface

defect sates. Defects create discrete electronic states and therefore influence optical properties.

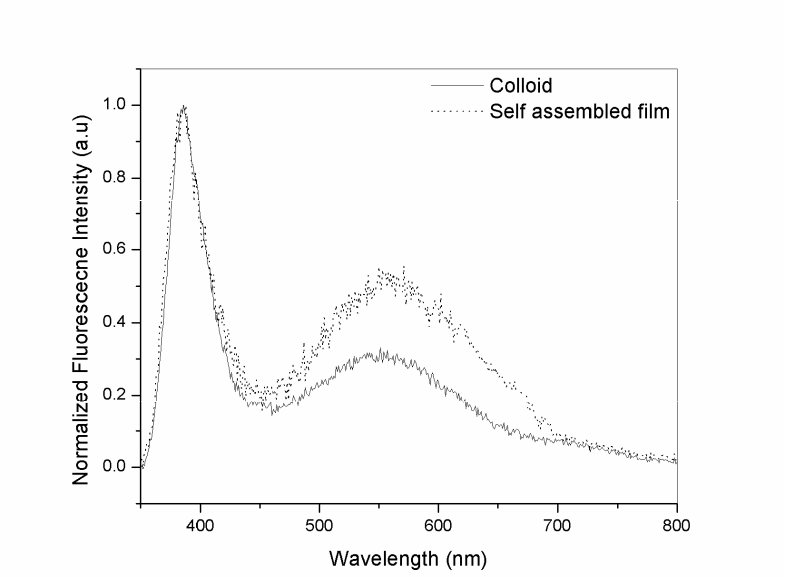

Figure 4.5: Fluorescence spectra of ZnO colloid and self assembled film for an excitation wavelength of 325 nm

4.9 Nonlinear optical characterization

One of the important applications of nano ZnO is in the field of photonic materials. The third order nonlinear optical properties of ZnO colloids and films are investigated using z-scan technique and are explained in chapter 3. Following studies describe the NLO properties of colloids and films of ZnO.

4.9.1 Open aperture z-scan

Typical results of the open aperture z-scan measurements of the films and colloid which correspond to the far-field normalized transmittance as a function of the distance from the lens focus at an intensity of 220 MW/cm^2 are shown in figure 4.6. The open aperture curve exhibits a

normalized transmittance valley, indicating the presence of induced absorption in the case of colloid and films which are developed by dip coating as well as pulsed laser ablation and a transmittance peak, indicating the presence of saturable absorption, in the case of self assembled film[16-17].

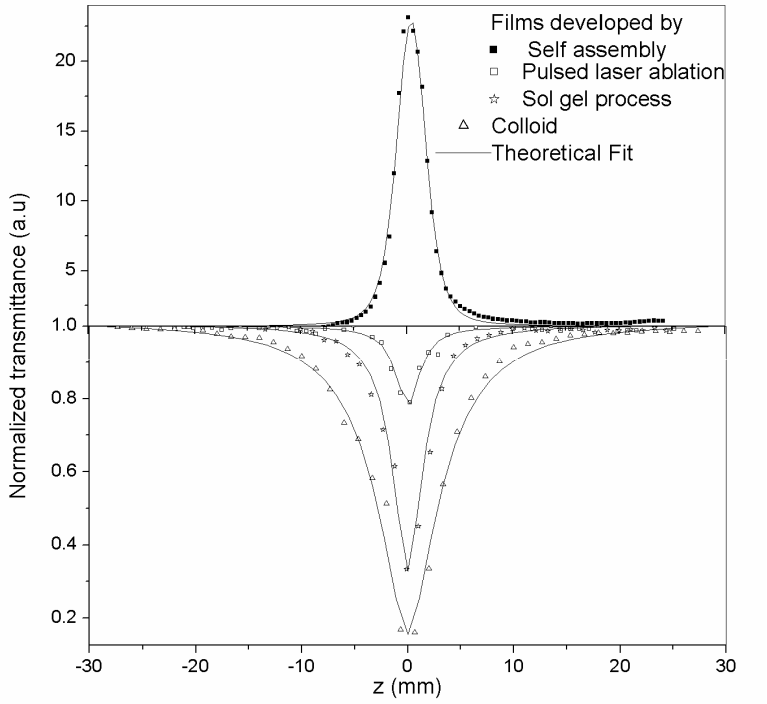

Figure 4.6: Open aperture z-scan traces of ZnO thin films and colloid at an intensity of 220 MW/cm^2 for an irradiation wavelength of 532 nm

In general, induced absorption can occur due to a variety of processes. The theory of two photon absorption process fitted well with the experimental curve infers that TPA is the basic mechanism and the possibility of free carrier absorption (FCA) contributing to induced absorption is explained in chapter 3. Considering all these factors and also that we used nanosecond excitation pulses, it is reasonable to assume that TPA followed by weak FCA are the important mechanisms contributing to

induced absorption in our colloid as well as dip coated and laser ablated samples[16-17].

The switching of saturable absorption behaviour in self assembled ZnO from induced absorption in colloidal ZnO is an interesting effect and can be used for applications such as optical pulse compression, optical switching and laser pulse narrowing[22]. The z-scan data shows that, along with moving the self assembled film towards the focus, the increase in the laser intensity induces saturation of the ground state absorption, which results in a transmittance increase (SA process).

The self assembled film exhibits saturation of absorption and bleaching and possesses a larger absorption coefficient than the other films and is more susceptible to thermal effects. For semiconductor materials, heat tends to reduce the fermi energy level and thereby, increase the number of carriers in the conduction band. This, in turn, depletes the ground level and induces bleaching in the ground state absorption, which results in SA process. The origin of optical nonlinearity is not only dependent on polarization response of bound electrons but also from conduction electrons in semiconductors. From figure 4.2, it is clear that the bandgap of the self assembled film is reduced to 3.1eV from that of the bulk (3.3 eV) and the laser intensity induces bleaching in the ground state absorption, which results in SA process. But the bandgap energies of the colloid and other 2 films are higher than the bulk which leads to induced absorption. These different nonlinear phenomena in the self assembled films can be attributed to the electronic transitions involving defect states[16-17].

The sensitivity of ZnO to impurities as well as native defects with respect to electronic properties is well known[23]. The breadth of the absorption edge of the self assembled film indicates that there are defect-related transitions in this case. The negative β value in ZnO thin films are

reported to be due to the saturated absorption of the defect states[23]. A similar explanation can hold for our self assembled films also. Thus the saturable absorption in self assembled films can be attributed to saturation of linear absorption of the ZnO defect states.

Generally ZnO exhibits induced absorption. In the self assembled film, the strong SA and the absence of induced absorption implies that the absorption cross-section of ground state is much larger than the absorption cross-section of excited state. All RSA materials possess a higher absorption cross-section of excited states compared to that of the ground state at the excitation radiation wavelength. Interestingly they will also give a positive value for the imaginary part of susceptibility $\mathrm{Im}\left(\chi^{(3)}\right)$ which is actually a measure of the induced absorption. On the other hand, a saturable absorber has a negative value for $\mathrm{Im}\left(\chi^{(3)}\right)$. The most important application of these materials is in optical limiting and to be used as protective material for sensitive devices.

4.9.2 Closed aperture z-scan

Figure 4.7 gives the closed aperture z-scan traces of ZnO colloid and films at an intensity of 220 MW/cm^2 for an irradiation wavelength of 532 nm. The closed aperture curve exhibited a peak to valley shape, indicating a negative value of the nonlinear refractive index n_2. The sign of nonlinear refractive index of all the samples remain negative whereas the absorptive nonlinearity reverses its sign when the material changes from colloid to self assembled film[16-17].

It is observed that the peak-valley of closed aperture z-scan satisfied the condition $\Delta z \sim 1.7\ z_0$, thus confirming the presence of pure electronic nonlinearity[24]. The major mechanism behind nonlinear refraction is two photon absorption and ZnO exhibits negative nonlinear refractive indices at 532 nm since the bandgap of bulk ZnO is 3.3 eV. It is reported that all

materials exhibit a sign change of the nonlinear refraction at about 2/3 of the bandgap[25]. There is no change in the sign of the nonlinear refractive index as the bandgap lies within the range 3.1-3.7 eV for the different samples and the sign change can be expected at near 600 nm. The SA in self assembled films can be attributed to bleaching of defect states and this does not affect the nonlinear refraction and hence there is no change in the sign of nonlinear refractive index whereas the absorptive nonlinearity for the self assembled film exhibits a trend which is reverse to that of the bulk. TPA always exists, even when saturable absorption appears to overlie this mechanism in self assembled films[16-17].

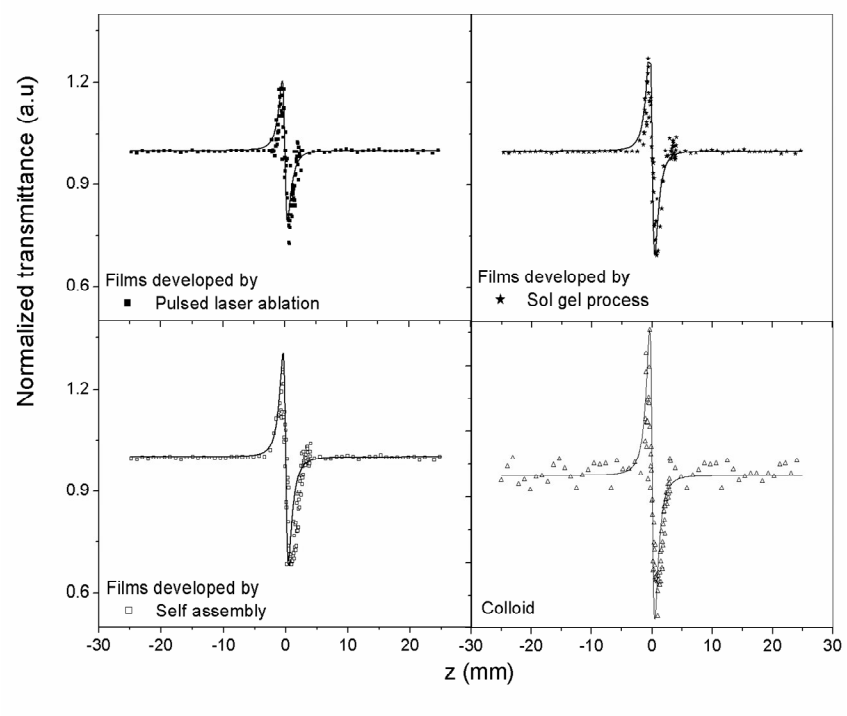

Figure 4.7: Closed aperture z-scan traces of ZnO thin films and colloid at an intensity of 220 MW/cm^2 for an irradiation wavelength of 532 nm

4.9.3 Nonlinear optical parameters

The nonlinear absorption coefficient, refractive index and third order susceptibility of ZnO films at an intensity of 220 MW/cm^2 for a wavelength of 532 nm are tabulated in table 4.1. When it is a saturable absorber, a more useful parameter to extract from the transmission measurements is the saturation intensity I_S, which is also given in the table[16-17]. These values are within an error of 7% contributed mainly by the uncertainty in intensity measurements on the sample and the fitting error.

Films developed by	β	I_S	n_2	$\mathrm{Im}\left(\chi^{(3)}\right)$	$\mathrm{Re}\left(\chi^{(3)}\right)$	$\left\|\chi^{(3)}\right\|$
	x10^{-5} m/W	GW/cm^2	x10^{-5} esu	x10^{-6} esu	x10^{-6} esu	x10^{-6} esu
Sol-gel process	4.6	-	-2.6	2.0	-5.5	5.9
Pulsed laser ablation	0.8	-	-1.9	0.3	-3.9	4.0
Self assembly	-	0.4	-2.8	-0.6	-5.9	5.9

Table 4.1: Measured values of nonlinear absorption coefficient, saturation intensity, nonlinear refractive index and third order susceptibility of ZnO films at an intensity of 220 MW/cm^2 for an irradiation wavelength of 532 nm

Based on these measurements we found that the imaginary part of the susceptibility is an order of magnitude smaller than the value for the real part of the susceptibility function. This means that the refraction effect is stronger than the absorption. One should be very careful while comparing the susceptibility values available in literature. These values vary to a great extent depending on the excitation wavelength, pulse duration, experimental

technique, concentration of the molecular species in the sample etc. The values of $\chi^{(3)}$ obtained for colloids are compared with the reported values in chapter 3. The values of $\chi^{(3)}$ measured at room temperature by femtosecond degenerate four wave mixing technique on ZnO microcrystalline thin films[26] range from 10^{-4} to 10^{-7} esu. The β values obtained are quite high, and are of the same order of magnitude as those obtained for ZnO-Cu and ZnO-Mg nanocomposite films[23, 27]. Thus, the real and imaginary parts of third order nonlinear optical susceptibility measured by the z-scan technique revealed that the ZnO colloid and films investigated here have good nonlinear optical response and could be chosen as ideal candidates with potential applications in nonlinear optics[16-17].

4.9.4 Size dependence

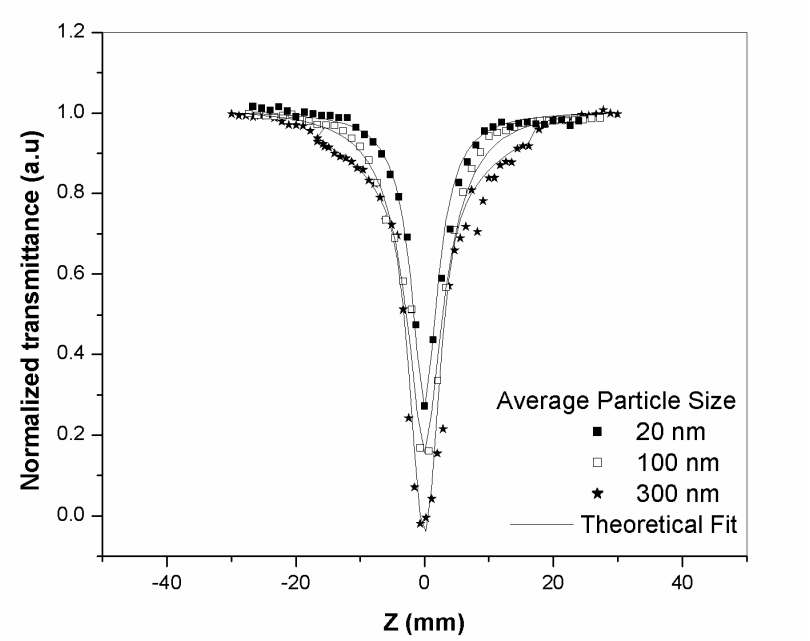

Figure 4.8(a): Open aperture z-scan traces of ZnO colloids of different particle sizes at an intensity of 220 MW/cm^2 for a wavelength of 532 nm

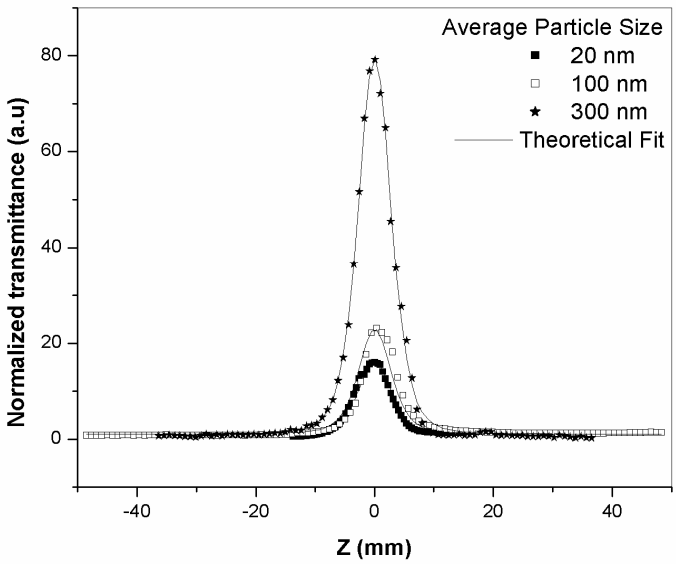

Figure 4.8(b): Open aperture z-scan traces of ZnO self assembled films of different particle sizes at an intensity of 220 MW/cm^2 for an irradiation wavelength of 532 nm

ZnO colloid and film for different particle sizes at an intensity of 220 MW/cm^2 for an irradiation wavelength of 532 nm are shown in figure 4.8 (a) and (b) respectively. The colloids exhibit RSA and the films show SA at all particle sizes from20-300 nm. The enhanced nonlinear optical properties of ZnO colloids with increase in particle size are due to strong two photon absorption. The susceptibility is size dependent, without showing a saturation behavior in the size range studied in our investigation[16]. The enhancement of nonlinear optical properties with increasing dimension in the weak confinement regime essentially originates from the size dependent enhancement of oscillator strength of coherently generated excitons and is explained in detail in chapter 3.

4.9.5 Fluence dependence

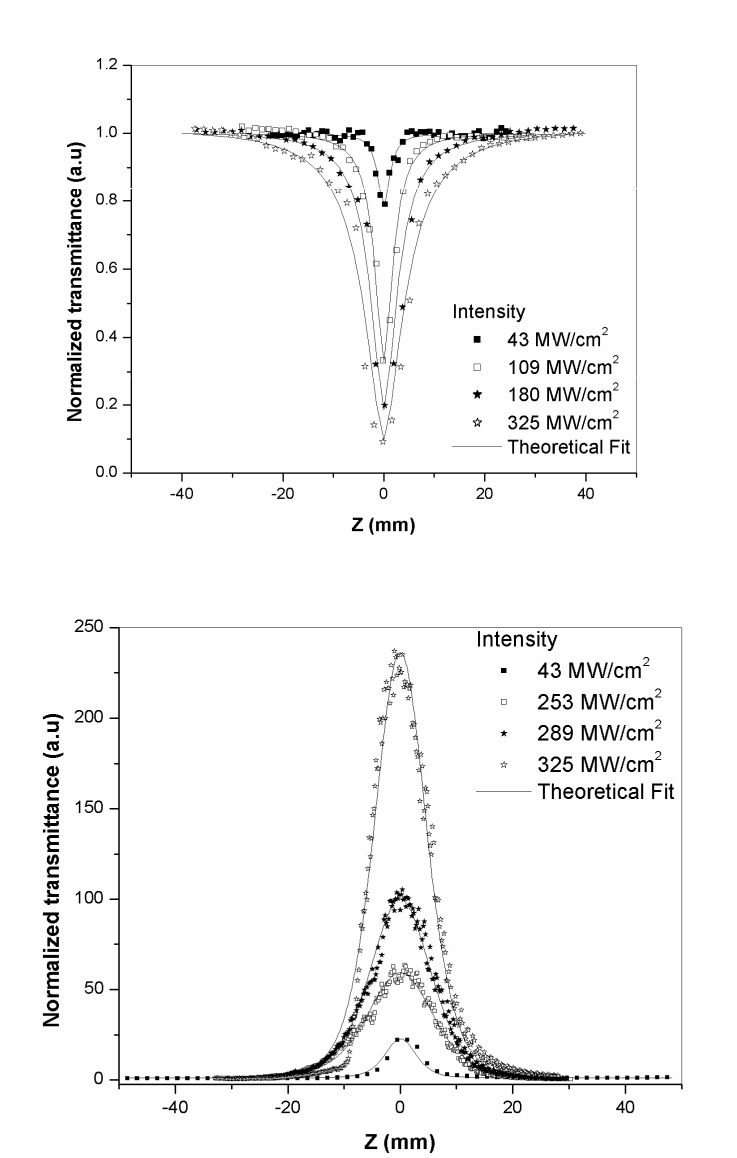

Figure 4.9: Open aperture z-scan curves of (a): ZnO colloid (b): ZnO self assembled films of size 300 nm at a wavelength of 532 nm for different irradiation intensities

The open aperture z-scan curves of ZnO colloid and self assembled film of size 300 nm at a wavelength of 532 nm for different irradiation intensities are shown in figure 4.9(a) and (b) respectively. We can see that nonlinear optical properties are highly irradiance dependent. The colloid shows induced absorption at all intensities under investigation. The results show three orders of enhancement from the reported value of 5cm/GW for bulk ZnO[28]. It has been reported that the reduced dimensionality of the particles resulted in considerable enhancement of the second-order susceptibility $\chi^{(2)}$ in thin films of ZnO[29]. Similar results in the third order nonlinear parameters are evident in our measurements also[16].

Now we will evaluate the saturation intensity of the self assembled film and attempt to interpret its SA behavior. We use the SA model described in equation (4.3) to fit our experimental open aperture z-scan trace displayed in figure 4.9(b), with only one adjustable parameter (I_S) and it is in good arrangement with the experimental data. The theoretical fitting give the respective I_S to be within a range of 0.12-0.52 GW/cm^2, for different intensity levels of I_0 ranging from 40 to 325 MW/cm^2 respectively. The results certainly imply that the self assembled films show only SA behavior[16]. It is well known that the theoretical model could describe the SA effect in a homogeneous broadening two level system very well. In the self assembled film, the strong SA and the absence of induced absorption imply that the absorption cross-section of ground state is much larger than the absorption cross-section of excited state.

4.9.6 Spectral dependence

The nature of nonlinear absorption in ZnO is dependent on the wavelength of the excitation beam[16]. It is seen that the material exhibits induced absorption for all wavelengths under investigation when it is in colloidal form.

(a)

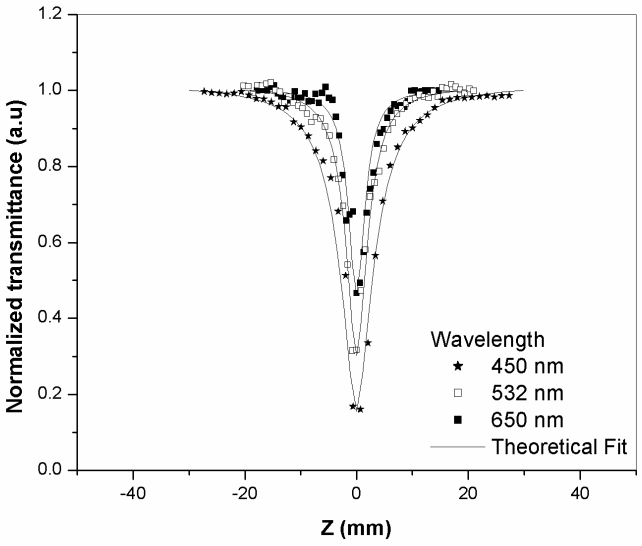

(b)

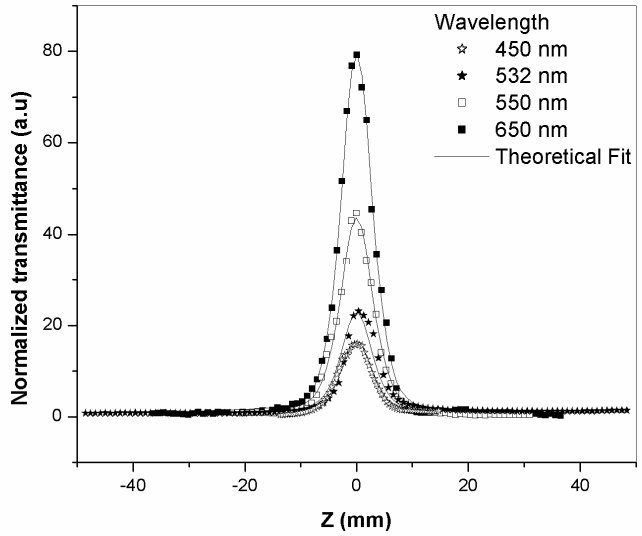

Figure 4.10: Open aperture z-scan curves of (a): ZnO colloid (b): ZnO self assembled films of size 300 nm at an intensity of 220 MW/cm^2 for different irradiation wavelengths

The self assembled film exhibits SA and the material does not exhibit any sign of absorptive nonlinearity for all wavelengths under investigation. This interesting feature is illustrated in figure 4.10 (a) and (b). However, it can be concluded that the nonlinear absorption changes from induced absorption to SA when the material changes from colloidal form to self assembled film.

4.9.7 Variation of imaginary part of susceptibility

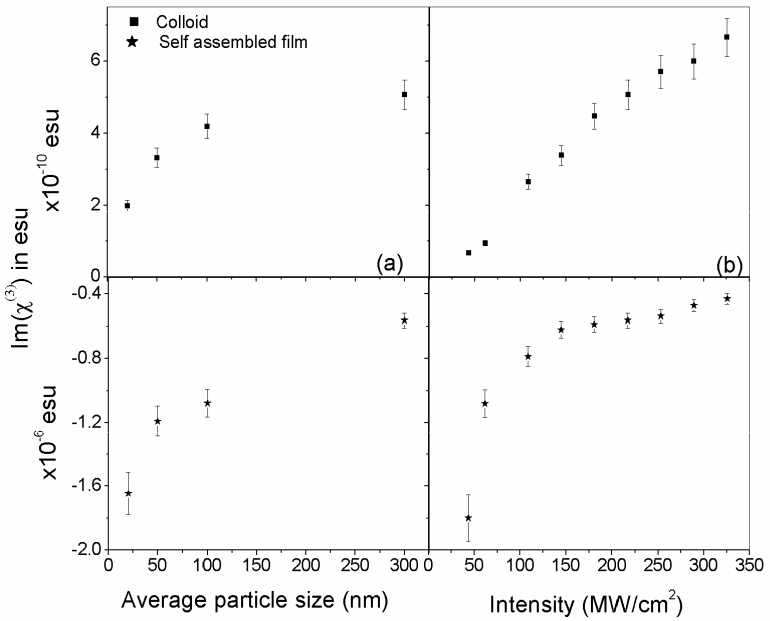

Figure 4.11: Vatriation of imaginary part of susceptibility with (a) Particle size (b) Intensity

All materials exhibiting RSA possess a higher absorption cross-section of excited states (σ_e) compared to that of the ground state (σ_g) at the excitation radiation wavelength[30]. Interestingly they will also give a positive value for the imaginary part of susceptibility $\mathrm{Im}\left(\chi^{(3)}\right)$ which is

actually a measure of the induced absorption. On the other hand, a saturable absorber has a negative value for $\mathrm{Im}(\chi^{(3)})$. The calculated values of $\mathrm{Im}(\chi^{(3)})$ as a function of size and intensity are shown in figure 4.11(a) and 4.10(b) respectively and it is found that susceptibility increases with particle size and intensity[16].

4.9.8 Figure of merit

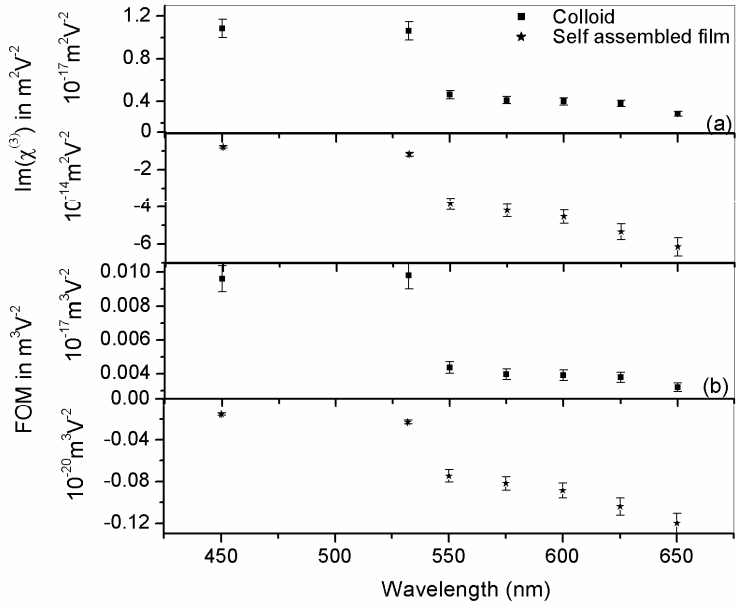

Figure 4.12:(a) Imaginary part of susceptibility as a function of wavelength (b) Figure of merit as a function of wavelength

The calculated values of $\mathrm{Im}(\chi^{(3)})$ as a function of wavelength are shown in figure 4.12(a). It will be useful to define a figure of merit (FOM) for these types of materials as the ratio $\mathrm{Im}(\chi^{(3)})/\alpha_0$, which specifies the magnitude of nonlinear absorption for unit value of linear absorption loss. FOM as a function of wavelength is plotted in figure 4.12(b) and it is found

that FOM is larger in the region between 450 and 550 nm. It helps in comparing the absorptive nonlinearities at various excitation wavelengths[16].

The most important application of these materials is in optical limiting and as a saturable absorber. Since these properties are spectral dependent, it is more common to use another figure of merit, σ_e / σ_g , which is the ratio of excited to ground state absorption cross-section. The value of σ_g can be obtained from the linear absorption spectrum using Beer's law. To evaluate σ_e we need to analyze the *z*-scan signal in a manner, as suggested by Wei *et al.*[31] and the work in the direction will be taken up as a future project.

4.10 Conclusions

ZnO colloids and self assembled films show two emission bands; an ultraviolet emission band and another in the green region. The presence of pronounced visible fluorescence in the self assembled film confirms the presence of surface defect sates. The nonlinear optical properties of self assembled films formed from ZnO colloidal spheres have been investigated and compared with those of films developed by sol-gel process and pulsed laser ablation using z-scan technique. ZnO colloids and thin films clearly exhibit a negative nonlinear index of refraction at 532 nm and the observed nonlinear refraction is attributed to two photon absorption followed by free carrier absorption. Although the absolute nonlinear values for these films are comparable, there is a change in absorptive nonlinearity of the films. The colloid and films developed by dip coating as well as pulsed laser ablation exhibit induced absorption whereas the self assembled film exhibits saturable absorption. This behaviour can be attributed to the saturation of linear absorption of the ZnO defect states. In the self assembled film, the strong SA and the absence of RSA implies that the absorption cross-section of ground state is much larger than the absorption cross-section of excited state. We

report our investigations of intensity, wavelength and size dependence of saturable and induced absorption of ZnO self assembled films and colloids. Values of the imaginary part of third order susceptibility are calculated for particles of size in the range 20-300 nm at different intensity levels ranging from 40 to 325 MW/cm^2 within the wavelength range of 450–650 nm. The wavelength dependence of figure of merit is calculated which helps in comparing the absorptive nonlinearities at various excitation wavelengths.

4.11 References

1 S. A. Studenikin, M. Cocivera, W. Kellner, and H. Pascher; "*Band-edge photoluminescence in polycrystalline ZnO films at 1.7 K*", J. Lumin. **91**, 223 (2000)

2 O. Painter, R.K. Lee, A. Scherer, A. Yariv, J.D. O'Brien, P.D. Dapkus and I. Kim; "*Two-Dimensional Photonic Band-Gap Defect Mode Laser*", Science **284**, 1819 (1999)

3 H.B. Sun, S. Matsuo and H. Misawa; "*Three dimensional photonic crystal structures achieved with two- photon-absorption photopolymerization of resin*", *Appl. Phys. Lett.* **74**, 786 (1999)

4 Eric W Seelig, Betty Tang, Alexey Yamilov, Hui Cao and R P H Chang; "*Self-assembled 3D photonic crystals from ZnO colloidal spheres*", Materials Chemistry and Physics **80**, 257 (2002)

5 S H Park, Y N Xia; "*Assembly of Mesoscale Particles over Large Areas and Its Application in Fabricating Tunable Optical Filters*", Langmuir **15**, 266 (1999)

6 S G Romanov, T Maka, C M S Torres, M Muller and R Zentel; "*Emission in a SnS2 inverted opaline photonic crystal*", Appl. Phys. Lett. **79**, 731 (2001)

7 K P Velikov and A van Blaaderen; "*Synthesis and Characterization of Monodisperse Core-Shell Colloidal Spheres of Zinc Sulfide and Silica"*, Langmuir **17**, 4779 (2001)

8 H Cao, J Y Xu, D Z Zhang, S H Chang, S T Ho, E W Seelig, X Liu and R P H Chang; "*Spatial Confinement of Laser Light in Active Random Media*", Phys. Rev. Lett. **84**, 5584 (2000)

9 N Fujimura, T Nishihara, S Goto, J Xu and T Ito; "*Control of preferred orientation for ZnO_x films: control of self-texture*", J. Cryst. Growth **130**, 269 (1993)

10 Lionel Vayssieres, Karin Keis, Sten-Eric Lindquist and Anders Hagfeldt; "*Purpose-Built Anisotropic Metal Oxide Material: 3D Highly Oriented Microrod Array of Zone",* J. Phys. Chem. B **105***,* 3350 (2001)

11 R. L. Sutherland, *Handbook of Nonlinear Optics,* Chap. 9 (Marcel Dekker, New York, 1996)

12 Y X Fan, J L He, Y G Wang, S Liu, H T Wang and X Y Ma; "*2-ps passively mode-locked Nd:YVO_4 laser using an output-coupling-type semiconductor saturable absorber mirro* ", Appl. Phys. Lett. **86**, 101103 (2005)

13 M S Bahae, A A Said, T H Wei, D J Hagan and E W Van Stryland; "*Sensitive measurement of optical nonlinearities using a single beam***",** *IEEE J. Quantum Electron*. **26**, 760 (1990)

14 B Gu, J Wang, J Chen, Y X Fan, J P Ding and H T Wang; "*Z-scan theory for material with two- and three-photon absorption*", Opt. Express **13**, 9230 (2005)

15 J He, W Ji, G H Ma, S H Tang, H I Elim, W X Sun, Z H Zhang and W S Chin; "*Excitonic nonlinear absorption in CdS nanocrystals studied using Z-scan technique*", J. Appl. Phys. **95**, 6381 (2004)

16 Litty Irimpan, A Deepthy, Bindu Krishnan, V P N Nampoori and P Radhakrishnan; "*Nonlinear optical characteristics of self assembled films of ZnO"* Applied Physics B*:* Lasers and Optics (2008), doi: 10.1007/s00340-007-2886-1

17 Litty Irimpan, A Deepthy, Bindu Krishnan, L M Kukreja, V P N Nampoori and P Radhakrishnan; "*Effect of self assembly on the nonlinear optical characteristics of ZnO thin films"* Optics Communications (2008) doi:10.1016/j.optcom.2008.01.029

18 D.L. Moreno, E.D. Rosa-Cruz, F.J. Cuevas, L.E. Regalado, P. Salas, R. Rodriguez and V.M. Castano; "*Refractive index measurement of pure and Er^{3+}-doped ZrO_2–SiO_2 sol–gel film by using the Brewster angle technique*", *Opt. Mat*. **19**, 275 (2002)

19 Lin Guo, Shihe Yang, Chunlei Yang, Ping Yu, Jiannong Wang, Weikun Ge, and George K. L. Wong; "H*ighly monodisperse polymer-capped ZnO nanoparticles: Preparation and optical properties",* Appl. Phys. Lett. **76**, 2901 (2000)

20 J G E Gardeniers, Z M Rittersm and G J Burger; "*Preferred orientation and piezoelectricity in sputtered ZnO films*", J. Appl. Phys. **83**, 7844 (1998)

21 A Kuroyanagi ; "*Properties of Aluminum-Doped ZnO Thin Films Grown by Electron Beam Evaporation*", Jpn. J. Appl. Phys. **28**, 219 (1989)

22 Y B Band, D J Harter and R Bavli; "*Optical pulse compressor composed of saturable and reverse saturable absorbers*", Chem. Phys. Lett. **126**, 280 (1986)

23 Ja-Hon Lin, Yin-Jen Chen, Hung-Yu Lin, and Wen-Feng Hsieh; "*Two-photon resonance assisted huge nonlinear refraction and absorption in ZnO thin films*" J. Appl. Phys. **97**, 033526 (2005)

24 M S Bahae, A A Said and E W van Stryland; "*High-sensitivity, single-beam n_2 measurements",* Opt. Lett. **14**, 955 (1989)

25 Sheik-Bahae, M Hutchings, D C Hagan, D J Van, Stryland E W; "*Dispersion of bound electron nonlinear refraction in solids*", IEEE JQE **27** (1991) 1296

26 W Zhang, H Wang, K S Wong, Z K Tang, G K L Wong and J Ravinder; *"Third-order*

optical nonlinearity in ZnO microcrystallite thin films", Appl. Phys. Lett. **75**,3321 (1999)

27 C S Suchand Sandeep, Reji Philip, R Satheeshkumar and V Kumar; "*Sol-gel synthesis and nonlinear optical transmission in* $Zn_{(1-x)}Mg_{(x)}O$ *(*$x \leq 0.2$*) thin films*" *Appl. Phys. Lett.* **89**, 063102 (2006)

28 *CRC Handbook of Laser Science and Technology: Optical Materials*, edited by M. J. Weber ~CRC Press, Boca Raton, FL, (1997)

29 Gang Wang, G T Kiehne, G K L Wong, J B Ketterson, X Liu, and R P H Chang, "*Large second harmonic response in ZnO thin films",* Appl. Phys. Lett., **80**, 401 (2002)

30 P J Gonalves, I E Borissevitch, L de Boni, N M Barbosa Neto, J J Rodrigues, Jr. and S C Zlio, XXVI Encontro Nacional de Física da Matétia Condensada, 2003 Caxambu. XXVI ENFMC-Annals of Optics, Vol. V5 (2003)

31 T H Wei, D J Hagan, M J Sence, E W Stryland, J W Perry and D R Coulter; "*Direct measurements of nonlinear absorption and refraction in solutions of phthalocyanines*", Appl. Phys. B: Lasers and optics **54**, 46 (1992)